



# Synthesis and Characterization of Pure Tin Oxide and Magnesium-doped Tin Oxide Nanoparticles by Chemical Precipitation Method

S. Kavitha\*, S. Sasikala, V. Kalaiselvi, V. Ramya

Department of Physics, Navarasam Arts & Science College for Women, Arachalur, Erode, TN, India

Received: 01.04.2020 Accepted: 04.05.2020 Published: 30-09-2020

\*kavivp12@gmail.com



## ABSTRACT

Magnesium-doped tin oxide ( $\text{SnO}_2$ ) nanoparticles were synthesized by the chemical precipitation method. This comes under bottom-up approach. The obtained results of metal oxide nanoparticles were characterized by XRD, FTIR, SEM, EDAX, UV and PL, respectively. The average grain size was calculated from XRD spectrum, which confirms the crystalline nature. Then the presence of functional groups was determined using Fourier Transform Infrared spectroscopy (FTIR), and surface morphology and particle size examinations were carried out by Scanning electron microscope (SEM). The purity and elemental composition of the sample were identified from EDAX. Finally, the optical properties and bandgap energy were analyzed by using UV-Visible spectroscopy and PL. It was concluded from the results that the samples synthesized were suitable for the application of dye degradation.

**Keywords:** Chemical precipitation method; Dye degradation; Mg-doped  $\text{SnO}_2$  nanoparticles; Pure  $\text{SnO}_2$ .

## 1. INTRODUCTION

Nanotechnology is a rapidly growing field of science and engineering due to the unique properties of nanoparticles, such as phase transition temperature, melting point and better solubility (Alivisatos *et al.* 1996). Nanotechnology has a wide range of uses in medicine, industry, material science, environmental science and other fields.  $\text{SnO}_2$  is a well-known n-type semiconductor with a large bandgap that is useful in gas sensors, solar cells, glass electrodes and secondary lithium batteries. It has a tetragonal rutile structure with n-type dopants in the form of inherent oxygen vacancies (Monredon *et al.* 2002). The efficiency of nanoparticles is directly proportional to their size, and thus has a strong correlation with the method of synthesis.

By reducing the size of  $\text{SnO}_2$  particles and/or adding dopants (typically noble metals or other metal oxides, such as  $\text{ZnO}$ ,  $\text{Nb}_2\text{O}_5$ ,  $\text{MnO}$ ,  $\text{Li}_2\text{O}$  and  $\text{Al}_2\text{O}_3$ ) to  $\text{SnO}_2$ , the system efficiency has been increased (Morales *et al.* 1999; Kumari *et al.* 2014). Due to the enhancement of properties when doped with Mg,  $\text{SnO}_2$  nanoparticles are considered possible materials for product fabrication. Because of its higher thermal solubility, Mg ion may be a promising choice to replace Sn ion in the  $\text{SnO}_2$  lattice. The ionic radius of  $\text{Mg}^{2+}$  is 72 nm, which is similar to the ionic radius of  $\text{Sn}^{4+}$ , which is 71 nm. As a result, replacing Sn with Mg has little effect on lattice constants or crystal structure (Wang *et al.* 2003). By doping  $\text{SnO}_2$

with a suitable Mg ratio, it could be possible to increase material efficiency and tune the energy band structure. Microwave-assisted solvothermal, polymeric intermediate, sol-gel hydrothermal, hydrothermal and chemical co-precipitation routes are among the methods used to make Mg-doped  $\text{SnO}_2$  nanoparticles (Nurul Syahidah Sabri *et al.* 2012). Co-precipitation is a straightforward technique for producing homogeneous nanoparticles for a variety of applications.  $\text{SnO}_2$ 's microstructure, morphology and luminescence efficiency are all highly dependent on the conditions under which it is prepared, which leads to a variety of possible applications (Nayral *et al.* 2000). The aim of this study is to design and test a co-precipitation method for Mg-doped  $\text{SnO}_2$  nanoparticles for a range of renewable energy applications.

## 2. MATERIALS & METHODS

### 2.1 Chemical synthesis of Pure and Mg-doped $\text{SnO}_2$

Co-precipitation is a simple, economical and industrially viable technique that can be used for the synthesis of oxide materials. Using this process, it is possible to prepare flowable powders without any additional agglomeration steps. One can tailor the process to get nano- or micron-size particles by adjusting the pH, the precipitating agent, temperature and solvents. This process has been successfully used for the

preparation of ceramic oxide powders suitable for suspension plasma spraying and powder plasma spraying.

## 2.2 Preparation of SnO<sub>2</sub> nanoparticles

6 g of tin oxide was dissolved in 200 ml distilled water, and the mixture was stirred for 20 minutes using a magnetic stirrer. Then few drops of Ammonia solution were added to the solution to maintain the pH level at 7. The mixture was stirred for 2 hours using a magnetic stirrer. The brown colour precipitate was obtained and filtered using Whatman No.1 filter paper to get a clear solution. It was kept in a microwave oven at 75 °C for 30 minutes, and again dried in a muffle furnace at 400 °C for 4 hours. The dried nanoparticles were taken in a mortar and made into a powder.

## 2.3 Precipitation of Mg-doped SnO<sub>2</sub> nanoparticles

6 g of tin oxide was dissolved in 100 ml distilled water and stirred for 1 hour using a magnetic stirrer. Then 0.207 g of magnesium was added to the above solution. The mixture was stirred for 1 hour. A few drops of Ammonia solution were added to maintain pH level at 7 and continuously stirred for 3 hours. Then the precipitate was collected, kept in a microwave oven at 75 °C for 30 minutes and then dried in a muffle furnace at 400 °C for 4 hours. The dried Mg-doped nanoparticles were taken in a mortar and into a powder.

## 3. CHARACTERIZATION TECHNIQUES

### 3.1 XRD Analysis

X-ray diffraction (XRD) is one of the most important non-destructive tools to analyze all kinds of matter, ranging from fluids to powders and crystals. It is a laboratory-based technique commonly used for the identification of crystalline materials and analysis of unit cell dimensions. This pattern predicts the lattice parameter, unit cell, volume and crystalline size of the sample. The mean crystalline size (D) of the particle was calculated from XRD line broadening measurement from the Debye-Scherrer formula.

$$D = K\lambda/\beta\cos \theta$$

where, D denotes the average crystalline size of the sample, K represents the broadening constant,  $\lambda$  denotes the wavelength of CuK $\alpha$  radiation source (1.54 Å),  $\beta$  represents full width at half-maximum and  $\theta$  denotes the angle of diffraction.

### 3.2 FTIR Analysis

Fourier transform infrared spectroscopy (FTIR) is an analytical technique used to identify organic (and in some cases inorganic) materials. This technique measures the absorption of infrared radiation by the sample material. The infrared absorption bands identify molecular components and structures. The FTIR spectrometer uses an interferometer to modulate the wavelength from a broadband infrared source. A detector measures the intensity of transmitted or reflected light as a function of its wavelength. The signal obtained from the detector is an interferogram, which must be analyzed with a computer using Fourier transforms to obtain a single-beam infrared spectrum. The frequency ranges are measured as wave numbers typically over the range of 4000 – 600 cm<sup>-1</sup>.

### 3.3 SEM and EDAX Analyses

The SEM analysis was used to investigate the size and morphology of pure and Mg-doped SnO<sub>2</sub> nanoparticles. Energy-dispersive X-ray spectroscopy (EDAX) is a qualitative and quantitative study; X-Ray micro-analytical technique can provide information on the chemical composition for elements and purity of the sample.

### 3.4 UV Spectroscopy

UV-Visible spectroscopy refers to absorption spectroscopy or reflectance spectroscopy in part of the ultraviolet and the full adjacent visible spectral regions (Warnken *et al.* 2001). It uses light in the visible and adjacent ranges. The absorption or reflectance in the visible range directly affects the perceived colour of the chemicals involved. In this region of the electromagnetic spectrum, atoms and molecules undergo electronic transitions. Absorption spectroscopy is complementary to fluorescence spectroscopy in that fluorescence deals with transitions from the excited state.

### 3.5 PL Analysis

Photoluminescence (PL) is the spontaneous emission of light from a material following optical excitation. It is a powerful technique to probe discrete energy levels and to extract valuable information about semiconductor sample composition, quantum well thickness or quantum dot sample mono-disparity.

## 4. RESULTS AND DISCUSSION

### 4.1 XRD Analysis

The X-ray powder diffraction (XRD) pattern of pure SnO<sub>2</sub> and Mg-doped SnO<sub>2</sub> nanoparticles were shown in Fig. 1. The XRD pattern confirms the crystalline structure with all possible peaks. The peaks in XRD pattern were observed at 2θ values, which correspond to the lattice planes 110, 101, 200, 211, 220 and 002 according to the database. XRD results have shown that Mg-doped SnO<sub>2</sub> grain size is higher than pure SnO<sub>2</sub> nanoparticles.

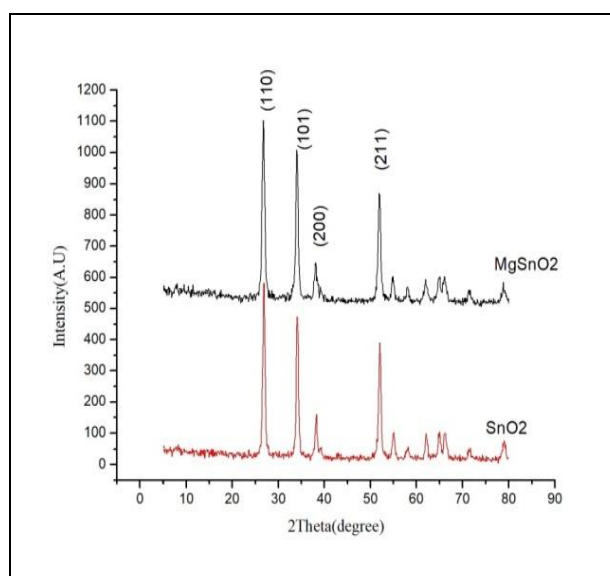


Fig. 1: XRD Patterns of Prepared Samples

Fig. 1 shows the typical patterns of pure and Mg-doped SnO<sub>2</sub> nanoparticles. The diffraction peaks of SnO<sub>2</sub> nanoparticles at 2θ = 26.7, 34.0, 39.2 and 64.8 are clearly distinguishable and could be indexed to the hkl planes are (110), (101), (111) and (211) tetragonal phases were observed. The results were in good agreement with the standard data file (JCPDS card No.: 41-1445). The calculated average crystalline size (D) of pure and Mg-doped SnO<sub>2</sub> nanoparticles is 14.02 nm and 13.45 nm. The crystalline size decreases for Mg-doped SnO<sub>2</sub> nanoparticles due to the concentration of doping material.

### 4.2 FTIR Analysis

The presence of functional groups in the samples has been analysed by using FTIR. Fig. 2 shows the spectra of pure and Mg-doped SnO<sub>2</sub> powder sample. The chemical structure of the synthesized nanoparticles was observed in the range of 400 cm<sup>-1</sup> to 4000 cm<sup>-1</sup>. The P-O stretching was confirmed from the observed peaks at 572 cm<sup>-1</sup>. CH<sub>3</sub> stretching was confirmed from the peak at 1000 cm<sup>-1</sup> and the peak at 3000 cm<sup>-1</sup> corresponds to C-H stretching.

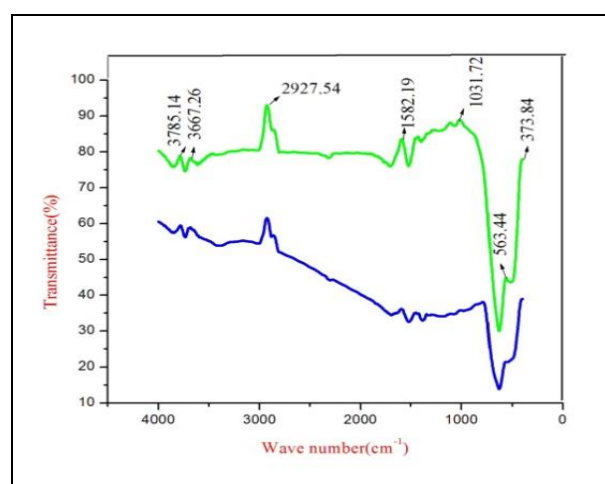


Fig. 2: FTIR Analyses of Pure and Mg-doped SnO<sub>2</sub> Nanoparticles

Table 1. XRD region of Pure SnO<sub>2</sub> and Mg-doped SnO<sub>2</sub> Nanoparticles

Sample	2θ (deg)	D spacing (Å)	Crystal size (nm)	Average crystal size (nm)
Pure SnO <sub>2</sub>	26.7999	3.32388	14.7788	14.0295
	34.0811	2.62858	14.7787	
	39.1000	2.30195	12.2940	
	64.9300	1.43503	14.2680	
Mg-doped SnO <sub>2</sub>	26.7094	3.33494	12.3227	13.4577
	34.0092	2.63397	12.7157	
	39.2000	2.29631	15.8115	
	64.8625	1.43636	12.9839	

Table 2. FTIR Analyses of Pure and Mg-doped SnO<sub>2</sub> Nanoparticles

S. No.	Sample	Wave number, cm <sup>-1</sup>				
		O-H stretching vibration	C-H stretching vibration	C=C stretching vibration	CH <sub>3</sub> stretching vibration	P-O Stretching vibration
1.	SnO <sub>2</sub>	3766.76	2918.88	1582.19	1338.86	563.44
2.	Mg-SnO <sub>2</sub>	3785.14	2927.54	1582.19	1411.31	563.44

### 4.3 SEM Analysis

Scanning electron microscopy was used to investigate the surface morphology and particle size of pure and Mg-doped SnO<sub>2</sub> nanoparticles. Fig. 3 shows the SEM images of the synthesized Mg-SnO<sub>2</sub>. It clearly reveals that both samples were spherical in shape and the particles were agglomerated. Finally, SEM image reveals that with the increase of doping concentration the grain size also increases.

### 4.4 EDAX Analysis

EDAX is used to identify the purity and composition of elements of the desired nanoparticles. Fig. 4.4 shows the presence of elements such as Sn (Tin) and O (Oxygen), which determines the pure tin oxide nanoparticles. Then Mg (Magnesium), Sn (Tin), O (Oxygen) represents the Mg-doped Sn nanoparticles.

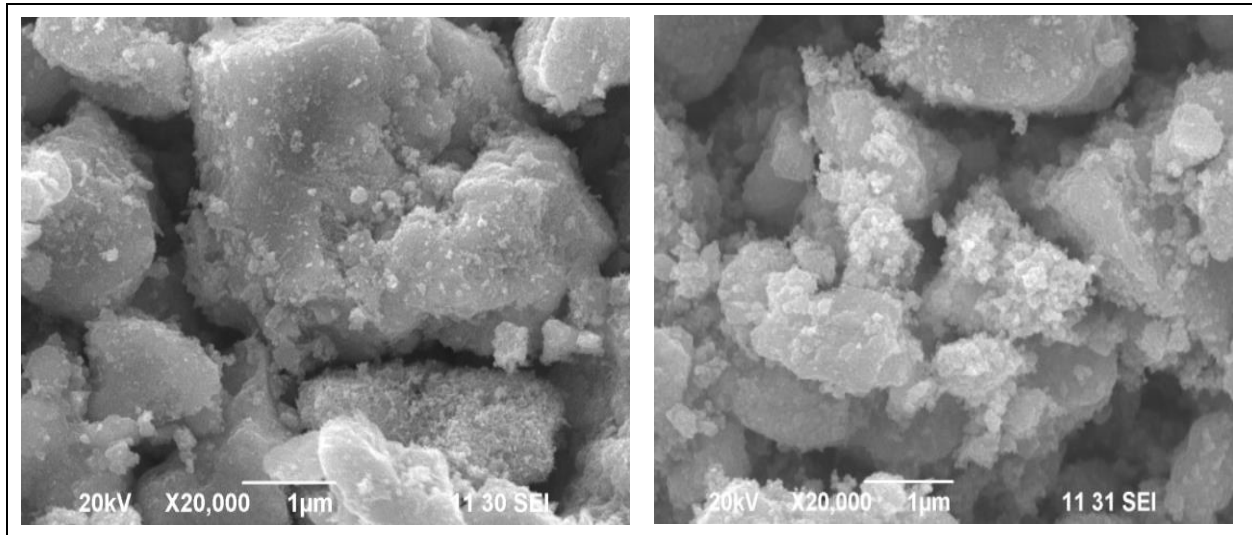


Fig. 3: SEM Analyses of Prepared Samples

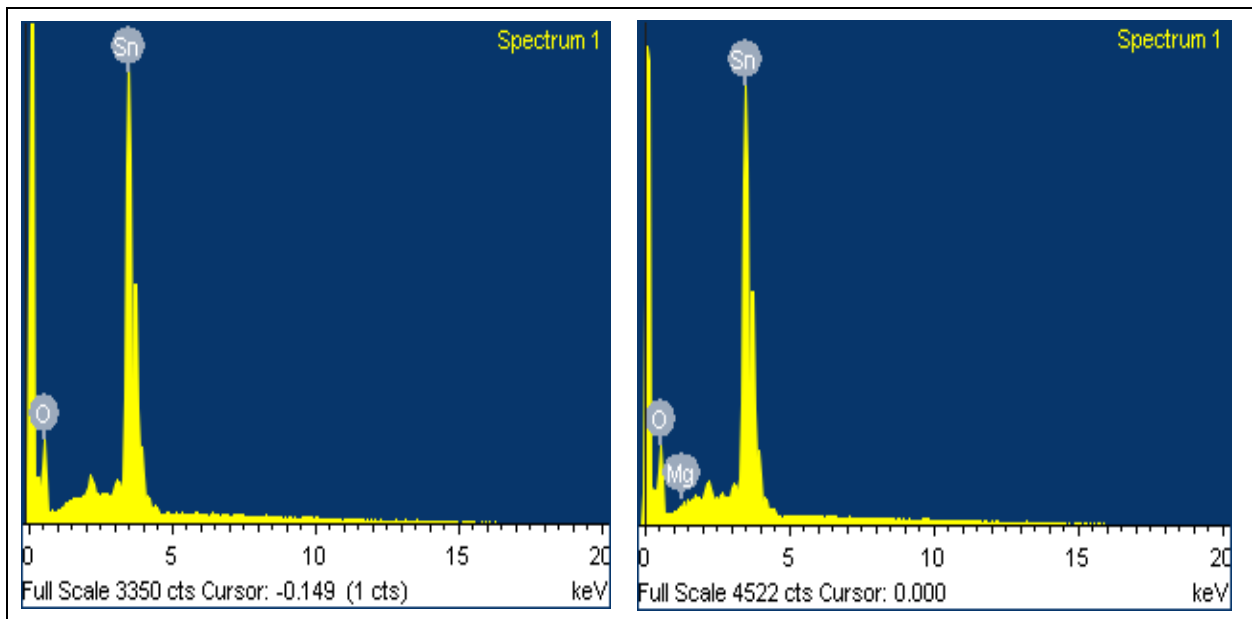


Fig. 4: EDAX Analyses of Prepared Samples

#### 4.5 UV Analysis

The UV-Visible spectra of pure SnO<sub>2</sub> and Mg-doped SnO<sub>2</sub> nanoparticles are shown in Fig. 5. The spectrum was recorded in the range of 200-800 nm. The absorbance peaks for both samples have a sharp peak in UV region. The bandgap energy of the sample can be predicted by the formula  $E_g = hc/\lambda$ . The absorption wavelength for pure tin oxide is 284 nm and for Mg-SnO<sub>2</sub> is 290 nm. The bandgap energies for pure and doped-tin oxide nanoparticles were 4.37 and 4.28 eV, respectively.

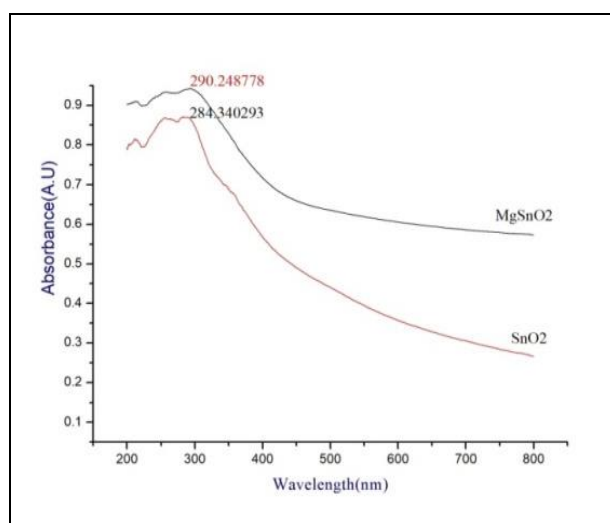


Fig. 5: UV Spectra of Prepared Samples

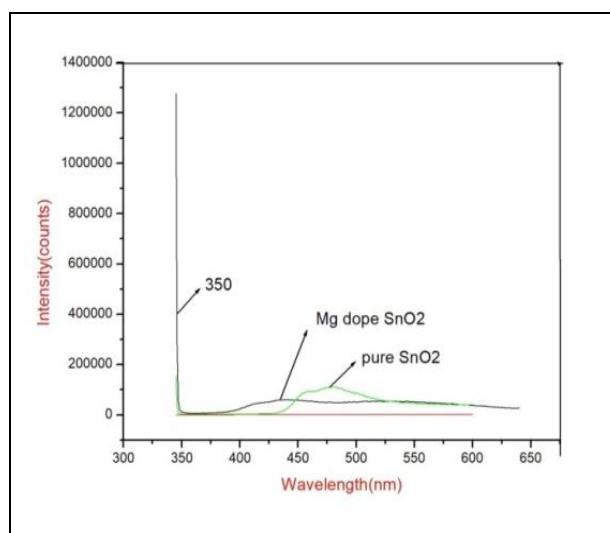


Fig. 6: PL Analyses of Prepared Samples

#### 4.6 Photo Luminescence Spectroscopy

The PL spectra of pure and Mg-doped SnO<sub>2</sub> nanoparticles were shown in Fig. 6. For Mg-doped SnO<sub>2</sub>, all peaks were slightly red-shifted, and the intensity of the peaks has also increased. The wavelength of the

spectrum for pure SnO<sub>2</sub> is 481 nm and Mg-doped SnO<sub>2</sub> is 436 nm.

#### 5. CONCLUSION

The present work deals with the synthesis and characterization of pure and Mg-doped SnO<sub>2</sub> nanoparticles. The XRD revealed the average crystalline size of pure SnO<sub>2</sub> nanoparticles as 14.02 nm and Mg-doped SnO<sub>2</sub> nanoparticles as 13.45 nm. The FTIR study determined the presence of functional groups in the sample. SEM has revealed that both samples have spherical shaped morphology and EDAX has shown the purity and elemental composition of the sample. Then UV and PL analyses have aided in investigating the optical properties, and the bandgap energies for pure and doped-tin oxide nanoparticles were found to be 4.37 and 4.28 eV, respectively.

#### FUNDING

This research received no specific grant from any funding agency in the public, commercial, or not-for-profit sectors.

#### CONFLICTS OF INTEREST

The authors declare that there is no conflict of interest.

#### COPYRIGHT

This article is an open access article distributed under the terms and conditions of the Creative Commons Attribution (CC-BY) license (<http://creativecommons.org/licenses/by/4.0/>).



#### REFERENCES

- Alivisatos, A. P., Semiconductor clusters, Nanocrystals, and Quantum Dots, *Science*, 271(5251), 933-937 (1996).  
<https://dx.doi.org/10.1126/science.271.5251.933>
- Kumari, N., Ghosh, A., Tewari, S. and Bhattacharjee, A., Synthesis, structural and optical properties of Al doped SnO<sub>2</sub> nanoparticles, *Ind. J. Phys.*, 88(1), 65-70 (2014).  
<https://dx.doi.org/10.1007/s12648-013-0387-0>
- Monredon, S. D., Cellot, A., Ribot, F., Sanchez, C., Armelao, L., Gueneau, L. and Delattre, L., Synthesis and characterization of crystalline tin oxide nanoparticles, *J. Mater. Chem.*, 12(8), 2396-2400 (2002).  
<https://dx.doi.org/10.1039/B203049G>



- Morales, J. and Sanchez, L., Electrochemical behaviour of SnO<sub>2</sub> doped with boron and indium in anodes for lithium secondary batteries, *Solid State Ion.*, 126(3-4), 219-226 (1999).  
[https://dx.doi.org/10.1016/S0167-2738\(99\)00251-9](https://dx.doi.org/10.1016/S0167-2738(99)00251-9)
- Nayral, C., Viala, E., Fau, P., Senocq, F., Jumas, J.C., Maisonnat, A. and Chaudret, B., Synthesis of tin and tin oxide nanoparticles of low size dispersity for application in gas sensing, *Chem. A Eur. J.*, 6(22), 4082-4090 (2000).  
[https://dx.doi.org/10.1002/1521-3765\(20001117\)6:22%3C4082::AID-CHEM4082%3E3.0.CO;2-S](https://dx.doi.org/10.1002/1521-3765(20001117)6:22%3C4082::AID-CHEM4082%3E3.0.CO;2-S)
- Nurul Syahidah Sabri, Mohd Salleh Mohd Deni, Azlan Zakaria and Mahesh Kumar Talari., Effect of Mn doping on structural and optical properties of SnO<sub>2</sub> nanoparticles prepared by mechanochemical processing, *Phys. Procedia*, 25, 233 – 239 (2012).  
<https://dx.doi.org/10.1016/j.phpro.2012.03.077>
- Wang, Y. and Lee, J. Y., Preparation of SnO<sub>2</sub> graphite nanocomposites anodes by ureamediated hydrolysis, *Electrochem. Commun.*, 5(4), 292-296 (2003).  
[https://dx.doi.org/10.1016/S1388-2481\(03\)00035-3](https://dx.doi.org/10.1016/S1388-2481(03)00035-3)
- Warnken, M., Lazark, K. and Wark, M., Redox behaviour of SnO<sub>2</sub> nanoparticles encapsulated in the pores of zeolites towards reductive gas atmospheres studied by in situ diffuse reflectance UV/Vis and Mossbauer spectroscopy, *Phys. Chem. Chem. Phys.*, 3(10), 1870-1876 (2001).  
<https://dx.doi.org/10.1039/B009045J>